

CHAPTER 19

Functional MR Imaging Using the BOLD Approach

Applications

Peter A. Bandettini, Jeffrey R. Binder, Edgar A. DeYoe, Stephen M. Rao, A. Jesmanowicz, Thomas A. Hammeke, Victor M. Haughton, Eric C. Wong, and James S. Hyde

Recent and fortuitous findings from the fields of human brain physiology and MR physics have precipitated the use of MRI for noninvasive mapping of human brain activation. Using radiotracer methods, Fox et al. observed in 1986 a highly localized decrease in oxygen extraction fraction (implying an increase in blood oxygenation) in regions of neuronal activation (1). Previously in 1982 Thulborn et al. had demonstrated that the T_2 of blood was increased by an increase in blood oxygenation (2). In 1990, it was subsequently discovered that MR signal in the vicinity of veins (3,4) and in brain parenchyma (5,6) was decreased by a decrease in blood oxygenation. This type of physiological contrast was named blood oxygenation level dependent (BOLD) contrast by Ogawa et al. (7). Hence, a mechanism for noninvasive imaging of activated regions in human brain became a possibility.

The use of BOLD contrast for the observation of brain activation was first demonstrated in August of 1991, at the tenth annual meeting of the Society of Mag-

netic Resonance in Medicine (8). The first papers demonstrating the technique, published in July 1992, reported human brain activation in the primary visual cortex (9,10) and motor cortex (9,11). In these experiments, a small but significant local signal increase in activated cortical regions was observed using susceptibility-weighted, gradient-echo pulse sequences.

The working model constructed to explain these observations was that an increase in neuronal activity caused local vasodilatation which, in turn, caused blood flow to increase. This resulted in an excess of oxygenated hemoglobin beyond the metabolic need, thus reducing the proportion of paramagnetic deoxyhemoglobin in the vasculature. This localized reduction in deoxyhemoglobin caused a reduction in microscopic B_0 field gradients in the vicinity of venules, veins, and red blood cells within veins, thereby causing an increase in spin coherence (increase in T_2 and T_2^*).

The physiological mechanisms which regulate cerebral hemodynamics and the precise manner in which the hemodynamic changes alter the MR signal are not completely understood. Other factors may cause changes in the apparent T_1 of activated tissue. These factors include activation-induced changes of blood inflow (12,13), and perfusion (9) rates. In general, the change in MR signal that accompanies neuronal activation is highly pulse sequence dependent. The dominant source of contrast in functional MRI (fMRI) will vary from flow changes to oxygenation changes and from larger vessels to smaller vessels, depending on the

P. A. Bandettini, A. Jesmanowicz, E. C. Wong, and J. S. Hyde: Biophysics Research Institute, Medical College of Wisconsin, Milwaukee, Wisconsin 53226.

J. R. Binder, S. M. Rao, and T. A. Hammeke: Department of Neurology, Medical College of Wisconsin, Milwaukee, Wisconsin 53226.

E. A. DeYoe: Department of Cellular Biology and Anatomy, Medical College of Wisconsin, Milwaukee, Wisconsin 53226.

V. M. Haughton: Department of Radiology, Medical College of Wisconsin, Milwaukee, Wisconsin 53226.

pulse sequence parameters. One can be confident that BOLD contrast is being observed when the pulse sequence is maximally T_2^* - or T_2 -weighted and minimally T_1 -weighted.

Despite these complexities, the application of BOLD contrast to mapping brain activation has several unique advantages that make the technique immediately useful. Because endogenous physiological contrast is used, the technique is completely noninvasive, thereby lending itself to extended or repeated use in single subjects. This permits the study of long term changes such as learning or habituation, and permits many experimental manipulations to be used. In addition, the BOLD contrast-to-noise ratio is high enough so that significant activation-induced signal changes may be observed in a single data set in 20 seconds.

fMRI has excellent spatial resolution. The upper limit of spatial resolution may be determined by the degree to which larger collecting veins contribute to the signal changes or cause artifactual signal changes. A concern is that collecting veins could show signal changes "downstream" from the actual region of activation. In addition, pulsatile artifacts are more likely to arise from larger vessels. Significant activation-induced signal changes may arise from both collecting veins and microvessels. If the contribution from larger collecting veins can be easily identified and/or eliminated, then, not only will the confidence in brain activation localization increase, but also the upper limits of spatial resolution will be determined by scanner resolution and BOLD contrast-to-noise ratio. Currently, voxel volumes as low as 1.2 microliters have been used (14), and experiments specifically devoted to probing the upper limits on functional spatial resolution have shown that fMRI can reveal activity localized to patches of cortex smaller than 1.5 mm (15).

The temporal resolution of fMRI is also relatively high. The hemodynamic response time, which is on the order of seconds (9,16,17), sets upper limits on the functional temporal resolution. Activation durations of less than a second are detectable (18,19) and relative differences (between adjacent regions or from different experiments) in the onset of signal enhancement are discriminable to within a second (20).

One other advantage of fMRI is the ease of registration of brain activation images with high resolution anatomical MR images. All brain activation images are directly registered with the images from the data set used to create them. In the same scanning session in which functional MRI time course series are obtained, other pulse sequences can be used to collect high resolution, high contrast anatomical images on which the activation images can be directly overlaid after possibly some unwarping. Three-dimensional brain activation data sets may also be obtained and fused directly with similar sets of high resolution anatomical images obtained during the same session. This information can

then be transformed into a common coordinate system [e.g., (21)], to aid the specification of the positions of activity foci within the brain. This transformation can be helpful for intrasubject averaging, but is also helpful for combining functional *and* anatomical MR data with information from other functional imaging techniques (19).

Owing to the advantages, ease of use, and accessibility of fMRI, many areas of the brain and many different tasks have already been studied. Primary cortical regions that have been studied with fMRI in addition to motor and visual cortex include the auditory cortex (22–27) and cerebellum (28–30). Regions activated by higher cognitive tasks have also been observed. Cognitive tasks have included word generation (31–33), mental imagery (34,36), mental rehearsal of motor tasks (37–39), complex motor control (36,37), higher visual processing (39–43), speech perception (25,44), single word semantic processing (44,45), working memory (46), and spatial memory (47). Subcortical activity (48) has also been observed during visual stimulation. Some further studies using fMRI have observed organizational differences related to handedness (49), and focal activity during seizures (50).

In this chapter, we demonstrate several applications of fMRI using BOLD contrast. Primary and higher order activity associated with the motor, visual, and auditory cortices are observed. Specifically, the following applications of fMRI using BOLD are shown: (i) Mapping of regions activated in the motor strip during finger, elbow, and toe movement. (ii) Mapping of regions associated with the performance and imagination of complex finger movement tasks. (iii) Mapping of the representation of the visual field in the primary visual cortex. (iv) Mapping of higher order areas beyond primary visual cortex activated by tasks involving visual discrimination and attention. (v) Mapping of regions in the auditory cortex associated specifically with speech recognition. (vi) Mapping of regions activated by reading and listening to spoken words.

GENERAL METHODOLOGY

All the studies presented in this chapter were performed using single shot 64×64 echo-planar imaging (EPI) on a standard 1.5 Tesla GE Signa scanner. To perform EPI without additional stress to the standard gradient amplifiers, we used an insertable balanced torque three-axis head gradient coil designed for rapid gradient switching (51). To obtain high quality images throughout the entire brain volume, a shielded quadrature elliptical endcapped transmit/receive birdcage radiofrequency coil (52) was used. The modular gradient-radiofrequency coil apparatus is illustrated in Figs. 1 and 2 (*see Color Plates 18 and 19 in color section*). Figure 1 (*Color Plate 18*) shows the radiofrequency coil removed from the gradient coil and Fig. 2 (*Color Plate*

19) shows the setup as it would appear before the subject and coil are placed into the magnet.

In all studies, sequential time series of susceptibility-weighted gradient-echo images ($TE = 40$ ms) were obtained. Single or multislice EPI was performed using time course series ranging from 64 to 1,024 images. The TR value used ranged from 0.3 to 3 seconds. The field of view was always 24 cm and the slice thickness ranged from 3 to 10 mm.

In all studies, brain activation tasks were presented in a repetitive on/off fashion for several cycles (from 2 to 12 cycles of approximately 8 to 20 seconds "off" and 8 to 20 seconds "on") throughout the EPI time course. Foci of brain activation were identified by cross correlation of the time course of each pixel with a reference wave form resembling the expected activation-induced response (53). Pixels having a temporal correlation coefficient below 0.4 to 0.6 were removed. After thresholding, the vector product of the reference waveform with each of the surviving time courses was calculated to yield an index of change in the signal magnitude. These "activation" images were then colorized and superimposed upon high resolution anatomical scans of the same slice obtained in the same imaging session.

SOMATOTOPIC MAPPING

Much of our current knowledge of the somatotopic organization of the primary motor cortex in humans is derived from the electrophysiological stimulation studies of Penfield et al. (54). The somatotopic organization of the primary motor cortex has been examined by positron emission tomography (PET) (55). A replication of this work with fMRI is needed because somatotopic organization of the motor cortex is well-defined and can serve as a validation of the technique. Alternatively, the results from electrical stimulation and PET studies may differ from those derived from imaging studies of voluntary movements observed using fMRI. This study presents findings using fMRI of primary motor cortex regions involved in the performance of simple motor tasks of finger, elbow, and toe flexion.

Eight right-handed subjects were imaged. Three contiguous coronal slices (slice thickness = 10 mm), containing the primary motor cortex, were selected for functional imaging. The head was flexed forward in the scanner relative to standard MR orientation (110° from the canthomeatal line) so as to align the middle slice with the precentral gyrus.

During each task, 104 consecutive images ($TR = 2$ s), were obtained during 10 alternating baseline and activation periods of 10 s each (20 seconds per on/off cycle). Activation tasks included simple, self-paced, repetitive flexion and extension movements of the right

fingers (digits 2–5 in unison), toes, and elbow. All pixels having a correlation coefficient value below 0.5 were removed. The functional images were interpolated to 256×256 resolution and superimposed upon 256×256 resolution anatomical scans obtained in the same imaging session.

Maximal functional activity was observed in the middle coronal slice, which most closely corresponded to the precentral gyrus. Figure 3 (*see Color Plate 20 in color section*) presents functional images for subjects 1 through 4, comparing finger and toe movements. No spatial overlap was observed between toe and finger activation locations. Toe movements produced signal changes within the interhemispheric fissure or on the lateral surface abutting the interhemispheric fissure, or both. Finger movements resulted in changes approximately two-thirds of the distance from the lateral fissure to the interhemispheric fissure. The areas of activation followed the gyral anatomy with almost all signal changes occurring within the gray matter either at the cortical surface or within the folds of the cortical gyri. Figure 4 (*see Color Plate 21 in color section*) compares finger and elbow movements for subjects 5–8. Signal intensity changes for elbow movements overlapped the more medial signal intensity changes observed with finger movements. The total area of activation was smaller for both toe and elbow movements relative to finger movements. Intersubject variability was present, possibly due to the variations in normal gyral anatomy as well as some variability in the selection of the brain slice locations. Occasional areas of activation were observed in subcortical regions adjacent to the third ventricle (subjects 1, 2, 5, and 6) or the insular region of the left hemisphere (subjects 3 and 5).

Results of this study suggest that fMRI has sufficient functional spatial resolution to demonstrate somatotopic organization of the primary motor cortex. In contrast to a previous PET study (55), the present fMRI investigation was able to distinguish arm from finger movements.

The cortical areas activated by voluntary movements appear to be somewhat larger than those described from electrical stimulation studies. This was particularly true for finger movements and may reflect the recruitment of muscle groups in the wrist and elbow during voluntary finger movements or the activation of areas within sulci that are not available to surface stimulation. Likewise, the "ankle" regions (on the lateral surface of the interhemispheric fissure) appear to be active in several subjects during toe movements. It is also possible that the active regions appear larger due to spatially removed collecting veins additionally contributing to the signal changes. Studies which have correlated fMRI results with electrical stimulation findings derived from patients undergoing intraoperative

cortical mapping have shown a correspondence only to within several millimeters (56).

A recent single cell recording study of primates taught to move individual fingers (57) has shown that the neuronal populations active with movements of different fingers overlap extensively. In preliminary data from our laboratory, we have also observed overlapping spatial patterns of activation for movements of individual fingers. These data suggest that traditional notions of somatotopic organization, derived from intraoperative electrical stimulation studies, may require revision when applied to the study of voluntary movements.

MAPPING OF COMPLEX MOTOR CONTROL

During the past decade, an increase in cerebral blood flow in the primary and non-primary motor cortex in response to voluntary movements has been demonstrated (58–65). In an influential study using the ^{133}Xe method, Roland et al. (63) showed that simple finger movements resulted in increases in regional cerebral blood flow confined to the contralateral sensorimotor hand region. In contrast, he showed that performance of a complicated finger sequencing task, while also producing an increase in cerebral blood flow in the contralateral sensorimotor area, produced a cerebral blood flow increase in the supplementary motor area and bilateral premotor cortex. Imagination of the complex finger task performance produced cerebral blood flow changes within the supplementary motor area, but not within the primary sensorimotor cortex.

Previous work in fMRI has demonstrated contralateral activation, and to a smaller degree, ipsilateral activation of the primary motor cortex, especially in the non-dominant hand (11,49,65). Recently, a study (36) has demonstrated additional activation in the supplementary motor area and bilaterally in the premotor cortex associated with the task of tapping out specified finger sequences, termed “complex” finger movements. Activation was also observed in the supplementary motor area during mental rehearsal of complex finger movement tasks.

In the present study, cortical and subcortical regions activated by simple, complex, and mental rehearsal of complex finger tapping paradigms were observed using extended time course (one slice) and multislice (whole brain) fMRI (37). All tasks were performed in a repetitive on/off manner. The on/off cycle length was 32 seconds. Simple finger movement involved tapping of fingers in no particular order against the patient table. Complex finger movement involved repetitively tapping out, for the duration of each activation time (16 seconds), a different five digit sequence (with numbers 1 through 5 representing each finger) presented at the

onset of every activation cycle. Mental rehearsal of complex finger movement was performed using the same digit presentation paradigm as with complex finger movement. During mental rehearsal, the subject was instructed not to move in any manner.

Single Slice Extended Time Course Analysis

In the single slice extended time course study, six finger movement paradigms were cyclically presented in six 320 second sections. Nine hundred and sixty axial images (slice thickness = 10 mm) of the same plane were collected (TR = 2 s). The total time course duration was 1,920 s (32 minutes). During each section, the subject performed the specific paradigm for ten on/off cycles. Figure 5 (*see Color Plate 22 in color section*) is a high resolution anatomical image of the slice selected for the study. The time course signals from the seven indicated regions are shown in Fig. 6, with the activation paradigm shown above each of the six sections.

Functional images, shown in Fig. 7 (*see Color Plate 23 in color section*), were created from the extended time course in the manner described in the general methodology section. The only difference was that the time course was divided into six sections corresponding to each paradigm, on each of which the cross correlation with a 160 point (320 second duration) reference waveform was calculated. Any pixels having a correlation coefficient below 0.4 were removed. The remaining pixels were used to create the brain activation images.

It is helpful to observe the time courses in Fig. 6 as well as the functional images in Fig. 7 (*Color Plate 23*) to obtain a better understanding of the spatial and dynamic characteristics of the signal changes corresponding with the particular tasks.

Regions 1 and 2 in Fig. 5 (*Color Plate 22*) are approximately in the left and right primary motor cortex. These regions demonstrated (Fig. 6) a strong and well-behaved cyclic response on the contralateral side during both the simple and complex finger movement tasks. A small negative correlation was observed during the imagined tasks (blue regions in the “imagined complex” images). It is hypothesized that tonic activation may actually have been inhibited in the primary motor cortex during imagination as the subject concentrated on *not* moving the fingers.

Regions 3 and 4 are approximately within in the left and right premotor cortex. Signal enhancement followed the time course during the complex and imagined complex tasks but not during the simple tasks. Also, the timing and amplitude of the activation-induced signal changes were not as high in amplitude nor as precisely time-locked as in the primary motor cortices. The functional images in Fig. 7 illustrate bilat-

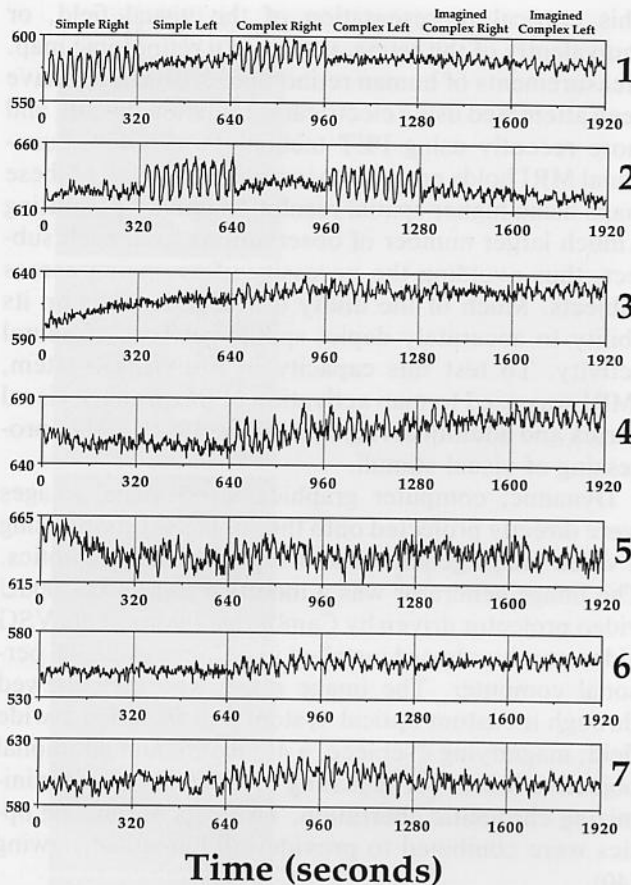


FIG. 6. Signal intensity versus time from the regions in Fig. 5 (*Color Plate 22*). The 32 minute-long time course was divided into six sections of 160 images each. During each of the six sections, the subject performed the specific paradigm, indicated at the top, for ten on/off cycles, lasting 32 seconds each. Regions in the primary motor cortex (1 and 2) showed well-behaved cyclic activation for the complex and imagined complex movement on the contralateral hand. Premotor (3 and 4), supplement (5), and posterior parietal (6 and 7) regions showed increased cyclic activity, bilaterally, during the performed and imagined complex finger movement sections.

eral activation of the premotor cortex during complex finger movement and imagined complex finger movement.

Region 5 is approximately in the supplementary motor area. The chosen slice may actually have been below most of the supplementary motor area, but activation-induced signal enhancement was still observed. It appears that the supplementary motor area was activated to some extent throughout the time course. The functional images in Fig. 7 also appear to show that complex and imagined complex finger movement caused more activation in the supplementary motor area than did the simple finger movement tasks.

Regions 6 and 7 are in the posterior parietal region. Simple finger movement caused no activation in these

regions, yet complex and imagined complex finger movement caused relatively strong signal changes. It is hypothesized that these regions may be related to attentional mechanisms or may be involved with finger positional planning. The regions are posterior and medial to the primary sensory cortices. The functional images in Fig. 7 illustrate that similar patterns of posterior parietal activation were manifested in the complex and imagined complex finger movement.

Several other aspects of the functional images in Fig. 7 are significant. Simple right finger movement caused mostly contralateral activation and minimal ipsilateral activation. Simple left finger movement caused a large amount of contralateral activation, but generally more ipsilateral activation. The cortical activation patterns with complex left and right finger movements differed only in the primary motor cortex region. Left and right complex finger movement demonstrated a similar activation pattern in the premotor, supplementary, and posterior parietal regions. Imagination of left and right finger movement resulted in similar cortical activation patterns regardless of the hand used. In addition, the pattern exhibited with imagination of the complex finger movement task was similar, other than in the primary motor cortex, to the complex finger movement task. One conclusion that can be made from this study is that imagined movements involve areas before the "final common pathway," beginning in the primary motor cortex. In addition, a strong inference is that the non-primary regions involved with planning, execution, and learning complex sequences of finger movement were the same regardless of the hand on which the task was performed.

Entire Brain Analysis

The use of single-shot EPI in combination with a TR of 2 seconds allows for the extension of single slice acquisition to as many as 20 slices with no compromise in total imaging time or image quality. In the study presented, finger movement tasks were cyclically presented in separate time course series (TR = 2 s) consisting of 100 images of each plane. The data set collected consisted of 10 sagittal slices (slice thickness = 8 mm) with an interplane spacing of 2 mm. For each of the time course series, a total of 1,000 images were collected. In each time course series, the subject alternated 16 s of activation with 16 s baseline for six on/off cycles. The paradigms performed were the same as those described in the previous section. For brevity, only the results from the time course series involving simple, complex, and imagined complex finger movement on the right hand are shown.

Figures 8–10 (*see Color Plates 24–26 in color section*) show high resolution anatomical images with re-

gions of activation superimposed in color. The slice sequence proceeds from a view of the left lateral aspect of the brain in panel 1 to the right lateral aspect in panel 10. Slices 5 and 6 straddle the midline, with slice 5 being positioned slightly closer to midline.

Figure 8 (*Color Plate 24*) shows activation with simple finger movement on the right hand. The contralateral motor cortex showed activation during simple finger movement. In addition, the cerebellum was activated on the ipsilateral side. Regions near the caudate nucleus of the basal ganglia also appeared to show activation. A small amount of activation was apparent in the supplementary motor area.

Figure 9 (*Color Plate 25*) shows activation with complex finger movement on the right hand. More extensive activation was apparent both anterior and posterior to the primary motor cortex. Activation was also more extensive in the cerebellum and supplementary motor area. Activation in the premotor region and in the posterior parietal region was bilateral.

Figure 10 (*Color Plate 26*) shows activation with imagination of complex finger movement. Activation was apparent in the supplementary motor area and cerebellum.

Results from the same imaging session involving finger movement tasks on the left hand (not shown) demonstrate similar results to those shown in the extended time course study. Non-primary regions activated during both complex finger movement and imagination of complex finger movement were common between hands.

We are able to perform entire brain fMRI primarily because of the high sensitivity quadrature coil used and the ability to easily obtain high B_0 homogeneity over a large volume at 1.5 Tesla. With the use of multislice EPI, a functional study of the entire brain involving an array of tasks and/or stimuli may be carried out in essentially the same amount of time as most standard clinical MRI scans.

Though susceptibility contrast is improved at higher field strengths, the pulse sequence, imaging hardware, system stability, and post-processing methodology also are extremely important in determining the quality of the brain activation images. From these results, it appears that susceptibility contrast is sufficient at 1.5 Tesla to carry out mapping of higher cognitive function in the human brain.

MAPPING THE REPRESENTATION OF THE VISUAL FIELD

In monkeys, it is known that there is a precise, topographic relationship between the position of a visual stimulus in the field of view and the position of the evoked activity in the primary visual cortex (66–68).

This cortical representation of the visual field, or equivalently of the retina, is termed a retinotopic map. Measurements of human retinotopic organization have been attempted using electrical stimulation (69,70), and more recently using PET technology (71–73). Functional MRI holds promise to increase the detail of these maps using higher spatial resolution and by permitting a much larger number of observations from each subject, thus avoiding the necessity of averaging across subjects. Much of the utility of fMRI depends on its ability to accurately depict spatial patterns of neural activity. To test this capacity in the visual system, fMRI was used to map activation of the primary visual cortex and additional regions involved with higher processing of visual stimuli.

Dynamic, computer graphics-based visual images were directly projected onto the subjects' retinæ using a video image generator and separate imaging optics. The image generator was a modified Sharp XG2000U video projector driven by Cambridge Instruments VSG video graphics board installed in a CompuAdd 386 personal computer. The image plane was then viewed through a custom optical system that included a wide field, magnifying eyepiece, a 45° prism, and additional objective lenses for adjusting magnification and minimizing chromatic aberration. Two sets of imaging optics were combined to provide full binocular viewing (40).

To map the retinotopic organization of the visual cortex, three highly trained subjects viewed a small white fixation dot on a uniform black or gray field subtending 60° of visual angle. A black and white checkered annulus surrounding the fixation point was presented for 5 on/off cycles of 10 s on and 10 s off. Time course series (TR = 2 s) of 100 images (slice thickness = 8 mm) were used. When on, the checkered pattern was either counter-phase modulated or flickered at 6–8 Hz. Three, four, or six successively larger annuli were tested. The width of each annulus as well as the check size were scaled in proportion to eccentricity. Functional images were obtained as described previously. Only pixels having a correlation coefficient of 0.55 or higher are shown.

Figure 11 illustrates the relative sizes of the annuli and shows the corresponding brain activation images. In these experiments, subjects passively viewed the stimuli and were not required to respond to them. A small checkerboard annulus presented at the fixation point elicited activation in striate cortex only at the occipital poles bilaterally. Annuli presented at increasing eccentricities activated successively more anterior regions of the calcarine sulcus. The most eccentric stimulus activated only the anterior calcarine cortex while sparing the occipital poles. Detailed examination of the sequence of activity foci in the left hemisphere (lower hemisphere in Fig. 11), shows a precise progres-

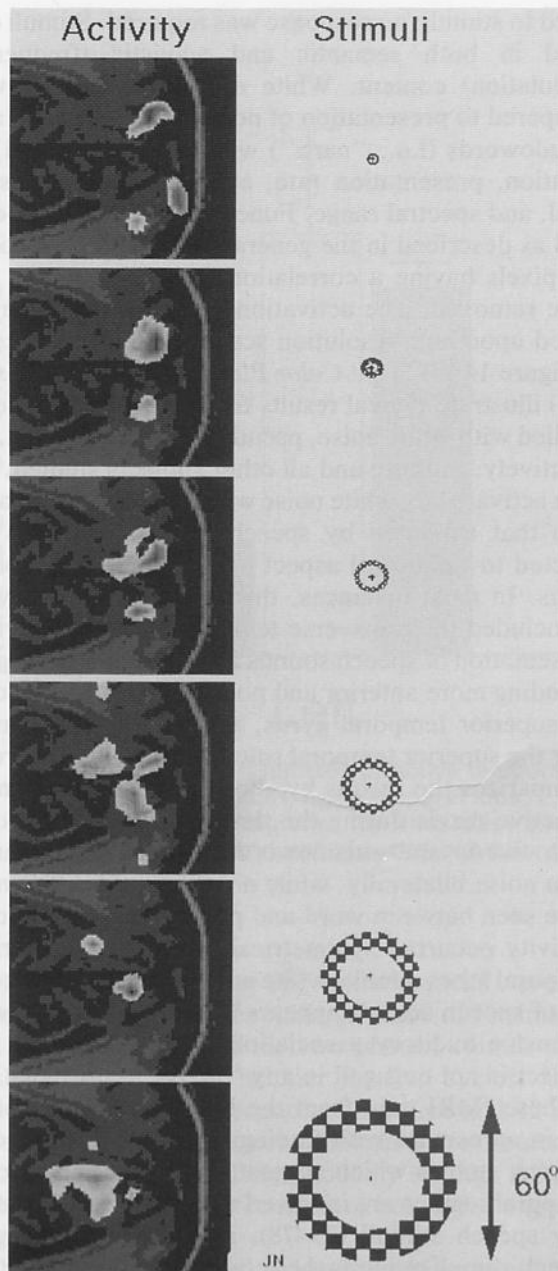


FIG. 11. Sagittal brain activation images created by passive viewing of visual stimuli with six different eccentricities while fixating at the center. The active foci traveled in an anterior direction along the calcarine fissure as the stimulus became more peripheral.

sion that closely followed the folded cortical mantle within the calcarine sulcus. While such a precise progression is not always observed, these data do show that under optimal conditions, a very detailed mapping of the visual field representation is possible with fMRI. It is certainly clear that resolution is not limited by the coarseness of the distribution of large blood vessels, even though such vessels may sometimes introduce artifacts.

Activation of the visual cortex during passive viewing was typically restricted to calcarine cortex, although additional variable foci were sometimes observed on the medial wall and lateral external surface of the occipital pole. To obtain more robust activation of additional visual areas beyond striate cortex, subjects were asked to discriminate and report the spatial configuration of additional target patterns superimposed on the checkerboard annuli. The target patterns consisted of groups of 1, 2, or 3 oval shapes represented by a check pattern that was spatially shifted relative to the checks of the annuli of Fig. 12 (see Color Plate 27 in color section). Successive presentations of the target patterns were either rotated around the annuli or mirror-reversed. The subject's task was to press a button to indicate if each new pattern was rotated or mirrored relative to the preceding pattern. During stimulus "on" periods, new target patterns were presented as fast as the subject could respond (typically every 2 to 4 s). During the blank control periods, subjects simply responded at random with approximately the same rate, though no stimulus, other than the fixation point was present on the screen.

Figure 12 (Color Plate 27) shows an example of differences in activation of extrastriate cortex during the passive viewing and active discrimination tasks. In this slice, discrimination caused robust activation along the occipitotemporal gyrus within a region that was well below primary visual cortex. This region was only weakly and variably active during passive viewing. Additional areas of increased activation were observed dorsal to the calcarine sulcus on the medial wall of the occipital lobe, and in the parietal and frontal cortex.

The use of an active discrimination task in conjunction with annuli of varying eccentricity permitted simultaneous assessment of the retinotopic organization of striate and extrastriate cortex. Figure 13 (see Color Plate 28 in color section) illustrates results from three axial sections either inferior to, within, or superior to the calcarine sulcus (top, middle, and bottom rows, respectively). Within each row is shown the activity evoked by successively more eccentric annuli. Dotted lines on either side of each section are approximately aligned with the major activity foci in each image. For calcarine and occipitotemporal cortex, a definite anterior shift of the foci was observed for annuli of increasing eccentricity. In contrast, a pair of small but consistent foci in the parieto-occipital cortex did not appear to shift, though some additional foci of activity did appear for the largest of the three annuli. Inspection of sagittal images of the occipital lobe from the same experiment (not illustrated) showed that nearly the entire medial wall was retinotopically organized with greater eccentricities represented more anteriorly. Approximate isoeccentricity contours were continuous and extended both dorsally and ventrally from the calcarine

sulcus. An additional distinct focus of activity showing possible retinotopic organization was observed on the lateral convexity of the brain at the approximate junction of the occipital, temporal, and parietal lobes.

These results demonstrate that higher order visual processing areas can be discerned, using fMRI, if appropriately designed discrimination tasks are used. In addition, these particular experiments demonstrate, for the first time, retinotopic organization of extrastriate visual areas beyond primary visual cortex.

AUDITORY SPEECH PERCEPTION

Since our initial report describing superior temporal gyrus activity during word presentation (22) our laboratory has initiated a number of fMRI studies involving auditory sensation and processing. These studies have included measurements of stimulus rate effects on signal changes in the auditory cortex (27), the identification of auditory cortical regions associated with speech perception (25), the identification of regions involved with single word semantic processing (44,45). We have also analyzed the spatially distributed phase variation in the activation-induced signal changes *within* the temporal lobe (20), and the latency differences *between* the temporal lobe and regions associated with semantic processing (26).

Passive sound presentation is interesting in that it emphasizes stimulus-dependent "automatic" processing of auditory stimuli and minimizes speech, motor, attentional, and memory activity. Pure tones and white noise differ inherently from speech in lacking many important acoustic cues relevant to speech perception. Among these is the absence of rapid frequency modulations which define component phonemic sounds in speech (74). The existence of these complex and rapidly changing acoustic elements in speech suggests that there may be cortical areas, presumably in or near the auditory association areas, that are primarily responsible for their analysis and identification. This study (25) presents findings using fMRI of brain regions involved in auditory speech perception. Specifically, regions activated by speech sounds (words and pseudowords) and non-speech sounds (noise) were compared.

Five right-handed subjects were tested. Symmetric lateral sagittal slices (slice thickness = 10 mm) of the left and right hemispheres were obtained, centered at positions 8 mm medial to the most lateral point of the temporal lobe on each side. In each time course series, 64 sequential images were collected (TR = 3 s), during which activation alternated with baseline every 9 s (6 images/cycle, 18 s/cycle, 10 cycles). During baseline periods, subjects heard only the ambient scanner noise. During activation periods, prepared digitized auditory stimuli were delivered. Subjects passively lis-

tened to stimuli; no response was required. Stimuli differed in both semantic and acoustic (frequency modulation) content. White noise presentation was compared to presentation of nouns (i.e., "barn"), and pseudowords (i.e., "narb") with stimuli matched for duration, presentation rate, average sound pressure level, and spectral range. Functional images were created as described in the general methodology section. All pixels having a correlation coefficient below 0.5 were removed. The activation images were superimposed upon high resolution scans of the same slices.

Figure 14A-C (*see Color Plate 29A-C in color section*) illustrate typical results from two of the subjects studied with white noise, pseudowords, and words, respectively. In these and all other subjects studied, the area activated by white noise was considerably smaller than that activated by speech sounds, and was restricted to the dorsal aspect of the superior temporal gyrus. In most instances, this region coincided with or included the transverse temporal (Heschl's) gyrus. Presentation of speech sounds activated a larger region including more anterior and posterior areas of the dorsal superior temporal gyrus, as well as cortex in or near the superior temporal sulcus bilaterally. Figure 15 summarizes the results by showing the mean number of active pixels during the three stimulus conditions. Both words and pseudowords differed significantly from noise bilaterally, while no significant differences were seen between word and pseudoword conditions. Activity occurred symmetrically in the left and right temporal lobes. Unlike white noise, therefore, processing of speech sounds appears to elicit participation of extensive auditory association areas even when the subject is not engaged in any "active" task.

These fMRI data from the human auditory cortex are in agreement with findings from other functional imaging studies which suggest that both left and right temporal regions are involved with processing of auditory speech stimuli (75-78), and that processing of speech stimuli requires the activity of more widespread brain areas than does processing of simpler non-speech sounds (79,80).

READING AND LISTENING TO WORDS

In the above sections, results from carefully controlled experiments regarding higher order motor, visual, and auditory function were presented. In this section, data from two uncontrolled pilot experiments are presented demonstrating the ease with which activation-induced signal changes can be obtained in single studies using equipment already in place in most clinical scanners (lights inside the bore and a patient intercom).

Two contiguous axial sections (slice thickness = 10

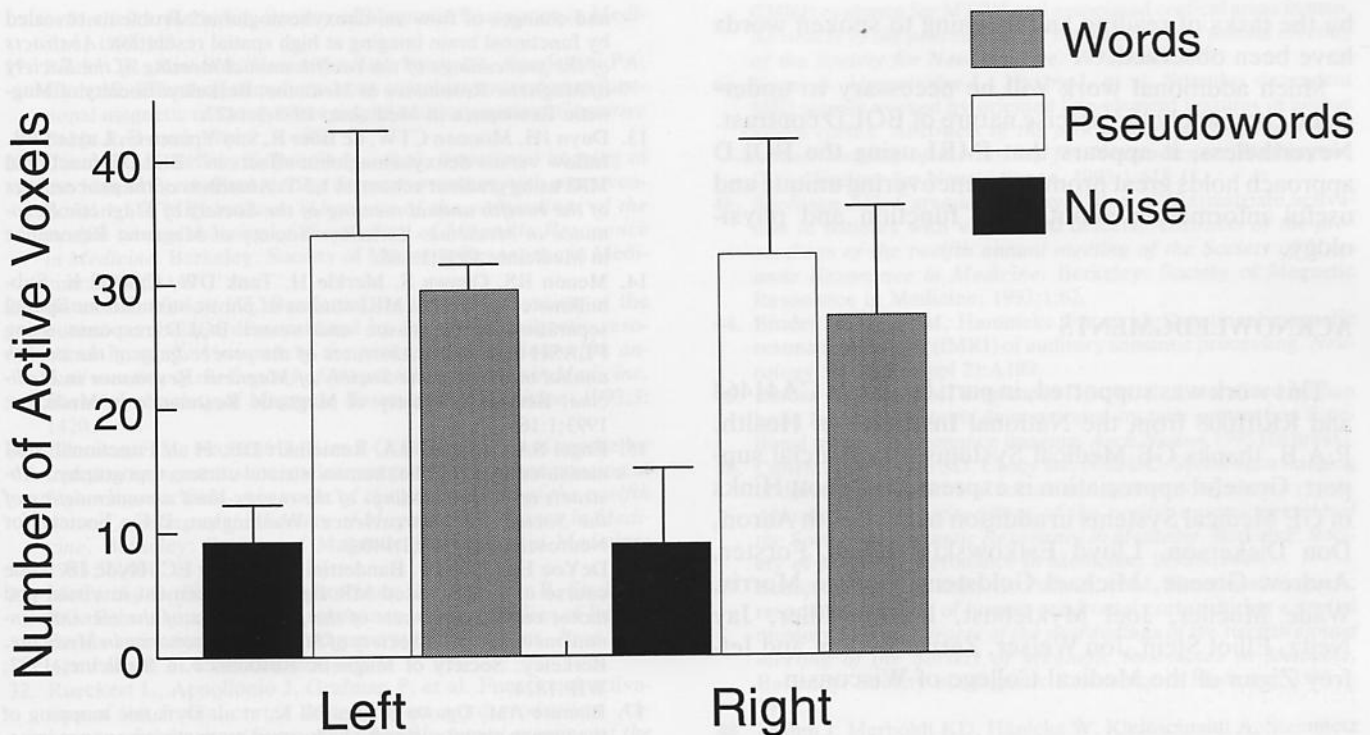


FIG. 15. Mean number of active temporal lobe pixels during three stimulus conditions in four subjects tested. R, right temporal lobe; L, left temporal lobe. Both word and pseudoword conditions differed significantly from noise bilaterally, while no significant differences were seen between word and pseudoword conditions. (From the American Neurological Association, with permission.)

mm) through the auditory and visual cortices were obtained. During the sequential acquisition of 128 images ($TR = 1$ s) for each of the two planes, stimuli were oscillated in an on/off manner for five cycles. Each cycle consisted of 12 seconds of baseline and 12 seconds of activation. Functional images were created as described in the general methodology section. All pixels having a correlation coefficient below 0.4 were removed.

The activation tasks consisted of either reading silently or listening to spoken words. During the baseline periods of both studies, the subjects lay with eyes closed. During the active state of the first study, the subject silently read text, using only the light inside the scanner for illumination. During the active state of the second study, the subject listened to single syllable words spoken through the patient intercom.

Figure 16A and B (see Color Plate 30A and B in color section) illustrate the activation images, through the same two sections, obtained by reading and listening to words, respectively. The area activated during the reading tasks covered a region extending from the primary visual cortex anteriorly to the temporal lobes. Bilateral temporal lobe activation was observed during the listening task. Between the tasks, some spatial overlap was observed in activated regions.

CONCLUSION

Functional MRI using BOLD contrast is a relatively new method for observing brain activation. Accompanying the novelty of the technique are many unknowns regarding the upper limits of spatial and temporal resolution as well as an unclear understanding of physiological and the biophysical mechanisms which regulate hemodynamic changes. In addition, the ways in which the hemodynamic changes affect the MR signal are incompletely understood. Nevertheless, the applications described here and elsewhere empirically establish the utility of this approach.

These studies have demonstrated applications of BOLD contrast based fMRI to the understanding of human brain activation. Regions activated in the motor cortex by movement of fingers, elbow, and toes have been mapped. Regions involved with performance and mental rehearsal of complex motor tasks have been imaged. The primary visual cortex has been retinotopically mapped, and retinotopic organization of some of the higher levels of the visual pathways have been observed. Differences have been observed in the temporal lobes during passive listening to white noise as opposed to speech sounds. Lastly, regions activated

by the tasks of reading and listening to spoken words have been observed.

Much additional work will be necessary to understand completely the precise nature of BOLD contrast. Nevertheless, it appears that fMRI using the BOLD approach holds great promise in uncovering unique and useful information about brain function and physiology.

ACKNOWLEDGMENTS

This work was supported, in part, by grants CA41464 and RR01008 from the National Institutes of Health. P.A.B. thanks GE Medical Systems for financial support. Grateful appreciation is expressed to Scott Hinks of GE Medical Systems in addition to Elizabeth Aaron, Don Dickerson, Lloyd Estkowski, Hubert Forster, Andrew Greene, Michael Goldstein, George Morris, Wade Mueller, Joel Myklebust, David Miller, Jay Neitz, Elliot Stein, Jon Weiser, Zerrin Yetkin, and Jeffrey Zigun of the Medical College of Wisconsin.

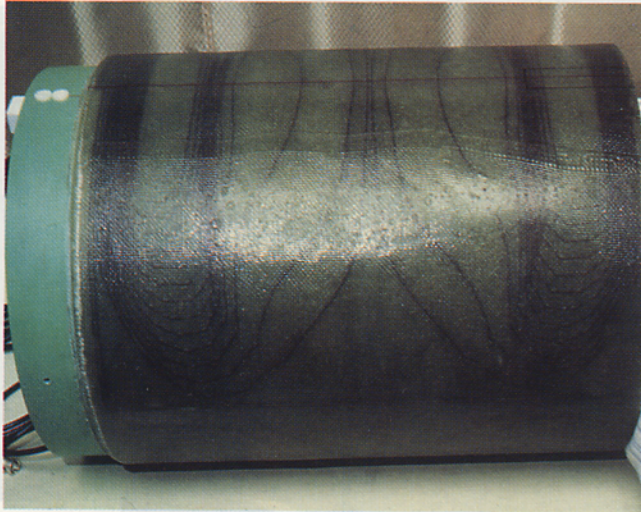
REFERENCES

1. Fox PT, Raichle ME. Focal physiological uncoupling of cerebral blood flow and oxidative metabolism during somatosensory stimulation in human subjects. *Proc Natl Acad Sci U S A* 1986; 83:1140-1144.
2. Thulborn KR, Waterton JC, Matthews PM, Radda GK. Oxygenation dependence of the transverse relaxation time of water protons in whole blood at high field. *Biochim Biophys Acta* 1982; 714:263-270.
3. Ogawa S, Lee TM, Nayak AS, Glynn P. Oxygenation-sensitive contrast in magnetic resonance imaging of rodent brain at high magnetic fields. *Magn Reson Med* 1990;14:68-78.
4. Ogawa S, Lee TM. Magnetic resonance imaging of blood vessels at high fields: *in vivo* and *in vitro* measurements and image simulation. *Magn Reson Med* 1990;16:9-18.
5. Turner R, LeBihan D, Moonen CT, Despres D, Frank J. Echo-planar time course MRI of cat brain oxygenation changes. *Magn Reson Med* 1991;22:159-166.
6. Hoppel BE, Weisskoff RM, Thulborn KR, Moore J, Rosen BR. Measurement of regional brain oxygenation state using echo planar linewidth mapping. *Abstracts of the proceedings of the tenth annual meeting of the Society of Magnetic Resonance in Medicine*. Berkeley: Society of Magnetic Resonance in Medicine; 1991;1:308.
7. Ogawa S, Lee TM, Kay AR, Tank DW. Brain magnetic resonance imaging with contrast dependent on blood oxygenation. *Proc Natl Acad Sci U S A* 1990;87:9868-9872.
8. Brady TJ. Future prospects for MR imaging. *Abstracts of the proceedings of the tenth annual meeting of the Society of Magnetic Resonance in Medicine*. Berkeley: Society of Magnetic Resonance in Medicine; 1991;1:2.
9. Kwong KK, Belliveau JW, Chesler DA, et al. Dynamic magnetic resonance imaging of human brain activity during primary sensory stimulation. *Proc Natl Acad Sci U S A* 1992;89:5675-5679.
10. Ogawa S, Tank DW, Menon R, et al. Intrinsic signal changes accompanying sensory stimulation: Functional brain mapping with magnetic resonance imaging. *Proc Natl Acad Sci U S A* 1992;89:5951-5955.
11. Bandettini PA, Wong EC, Hinks RS, Tikofsky RS, Hyde JS. Time course EPI of human brain function during task activation. *Magn Reson Med* 1992;25:390-397.
12. Frahm J, Merboldt KD, Hänicke W. Tissue vs. vascular effects and changes of flow vs. deoxyhemoglobin? Problems revealed by functional brain imaging at high spatial resolution. *Abstracts of the proceedings of the twelfth annual meeting of the Society of Magnetic Resonance in Medicine*. Berkeley: Society of Magnetic Resonance in Medicine; 1993;3:1427.
13. Duyn JH, Moonen CTW, de Boer R, van Yperen G, Luyten PR. Inflow versus deoxyhemoglobin effects in "BOLD" functional MRI using gradient echoes at 1.5 T. *Abstracts of the proceedings of the twelfth annual meeting of the Society of Magnetic Resonance in Medicine*. Berkeley: Society of Magnetic Resonance in Medicine; 1993;1:168.
14. Menon RS, Ogawa S, Merkle H, Tank DW, Ugürbil K. Submillimeter functional MRI studies of photic stimulation: Spatial separation of the tissue and vessel BOLD response using FLASH at 4 Tesla. *Abstracts of the proceedings of the twelfth annual meeting of the Society of Magnetic Resonance in Medicine*. Berkeley: Society of Magnetic Resonance in Medicine; 1993;1:165.
15. Engel SA, Wandell BA, Rumelhart DE, et al. Functional MRI measurements of the human striate cortex topography. *Abstracts of the proceedings of the twenty-third annual meeting of the Society for Neuroscience*. Washington, D.C.: Society for Neuroscience, 1993;1:140.8.
16. DeYoe EA, Neitz J, Bandettini PA, Wong EC, Hyde JS. Time course of event-related MR signal enhancement in visual and motor cortex. *Abstracts of the proceedings of the eleventh annual meeting of the Society of Magnetic Resonance in Medicine*. Berkeley: Society of Magnetic Resonance in Medicine; 1992; WIP:1824.
17. Blamire AM, Ogawa S, Ugürbil K, et al. Dynamic mapping of the human visual cortex by high speed magnetic resonance imaging. *Proc Natl Acad Sci U S A* 1992;89:11069-11073.
18. Bandettini PA, Wong EC, DeYoe EA, et al. The functional dynamics of blood oxygenation level dependent contrast in the motor cortex. *Abstracts of the proceedings of the twelfth annual meeting of the Society of Magnetic Resonance in Medicine*. Berkeley: Society of Magnetic Resonance in Medicine; 1993;3:1382.
19. Belliveau JW, Baker JR, Kwong KK, et al. Functional neuroimaging combining fMRI, MEG, and EEG. *Abstracts of the proceedings of the twelfth annual meeting of the Society of Magnetic Resonance in Medicine*. Berkeley: Society of Magnetic Resonance in Medicine; 1993;1:6.
20. Binder JR, Jesmanowicz A, Rao SM, et al. Analysis of phase differences in periodic functional MRI activation data. *Abstracts of the proceedings of the twelfth annual meeting of the Society of Magnetic Resonance in Medicine*. Berkeley: Society of Magnetic Resonance in Medicine; 1993;3:1383.
21. Tailairach J, Szikla G, Tournoux P, et al. *Atlas d'anatomie stereotaxique du telencephale*, 1st ed. Paris: Masson; 1967.
22. Rao SM, Bandettini PA, Wong EC, et al. Gradient-echo EPI demonstrates bilateral superior temporal gyrus activation during passive word presentation. *Abstracts of the proceedings of the eleventh annual meeting of the Society of Magnetic Resonance in Medicine*. Berkeley: Society of Magnetic Resonance in Medicine; 1992;WIP:1827.
23. Singh M, Kim H, Kim T, Khosla D, Colletti P. Functional MRI at 1.5 T during auditory stimulation. *Abstracts of the proceedings of the twelfth annual meeting of the Society of Magnetic Resonance in Medicine*. Berkeley: Society of Magnetic Resonance in Medicine; 1993;3:1431.
24. Turner R, Jezzard P, LeBihan D, Prinster A, Pannier L, Zeffiro T. BOLD contrast imaging of cortical regions used in processing auditory stimuli. *Abstracts of the proceedings of the twelfth annual meeting of the Society of Magnetic Resonance in Medicine*. Berkeley: Society of Magnetic Resonance in Medicine; 1993;3:1411.
25. Binder JR, Rao SM, Hammeke TA, et al. Functional magnetic resonance imaging of human auditory cortex. *Ann Neurol* 1994; 35:662-672.
26. Binder JR, Rao SM, Hammeke TA, et al. Temporal characteristics of functional magnetic resonance signal change in lateral frontal and auditory cortex. *Abstracts of the proceedings of the twelfth annual meeting of the Society of Magnetic Resonance*

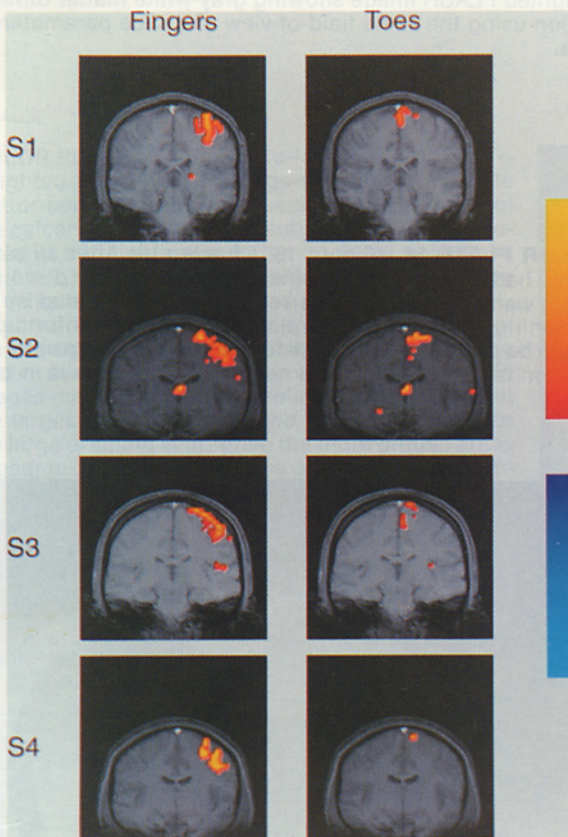
- in Medicine. Berkeley: Society of Magnetic Resonance in Medicine; 1993;1:5.
27. Binder JR, Rao SM, Hammeke TA, Frost JA, Bandettini PA, Hyde JS. Effects of stimulus rate on signal response during functional magnetic resonance imaging of auditory cortex. *Cognitive Brain Research* 1994;2:31-38.
 28. Cuenod CA, Zeffiro T, Pannier L, et al. Functional imaging of the human cerebellum during finger movement with a conventional 1.5 T MRI scanner. *Abstracts of the proceedings of the twelfth annual meeting of the Society of Magnetic Resonance in Medicine*. Berkeley: Society of Magnetic Resonance in Medicine; 1993;3:1421.
 29. Bates SR, Yetkin FZ, Bandettini PA, et al. Activation of the human cerebellum demonstrated by functional magnetic resonance imaging. *Abstracts of the proceedings of the twelfth annual meeting of the Society of Magnetic Resonance in Medicine*. Berkeley: Society of Magnetic Resonance in Medicine; 1993;3:1420.
 30. Ellermann JM, Flament D, Kim S-G, et al. Studies of cerebellar function using multislice nuclear magnetic resonance imaging at high magnetic field. *Abstracts of the proceedings of the twelfth annual meeting of the Society of Magnetic Resonance in Medicine*. Berkeley: Society of Magnetic Resonance in Medicine; 1993;3:1401.
 31. McCarthy G, Blamire AM, Rothman DL, Gruetter R, Shulman RG. Echo-planar magnetic resonance imaging studies of frontal cortex activation during word generation in humans. *Proc Natl Acad Sci U S A* 1993;90:4952-4956.
 32. Rueckert L, Appollonio J, Grafman P, et al. Functional activation of left frontal cortex during covert word production. *Abstracts of the proceedings of the twelfth annual meeting of the Society of Magnetic Resonance in Medicine*. Berkeley: Society of Magnetic Resonance in Medicine; 1993;1:60.
 33. Hinke RM, Hu X, Stillman AE, Ugurbil K. The use of multislice functional MRI during internal speech to demonstrate the lateralization of language function. *Abstracts of the proceedings of the twelfth annual meeting of the Society of Magnetic Resonance in Medicine*. Berkeley: Society of Magnetic Resonance in Medicine; 1993;1:63.
 34. Le Bihan D, Turner R, Jezard P, Cuenod CA, Zeffiro T. Activation of human primary visual cortex during visual recall: A magnetic resonance imaging study. *Proc Natl Acad Sci U S A* 1993;90:11802-11805.
 35. Menon R, Ogawa S, Tank DW, et al. Visual mental imagery by functional brain MRI. *Abstracts of the proceedings of the twelfth annual meeting of the Society of Magnetic Resonance in Medicine*. Berkeley: Society of Magnetic Resonance in Medicine; 1993;3:1381.
 36. Rao SM, Binder JR, Bandettini PA, et al. Functional magnetic resonance imaging of complex human movements. *Neurology* 1993;43:2311-2318.
 37. Bandettini PA, Rao SM, Binder JR, et al. Magnetic resonance functional neuroimaging of the entire brain during performance and mental rehearsal of complex finger movement task. *Abstracts of the proceedings of the twelfth annual meeting of the Society of Magnetic Resonance in Medicine*. Berkeley: Society of Magnetic Resonance in Medicine; 1993;3:1396.
 38. Takahashi T, Takiguchi K, Itagaki H, et al. Real time imaging of brain activation during imagination of finger tasks. *Abstracts of the proceedings of the twelfth annual meeting of the Society of Magnetic Resonance in Medicine*. Berkeley: Society of Magnetic Resonance in Medicine; 1993;3:1415.
 39. Schneider W, Casey BJ, Noll D. Functional MRI mapping of individual stages of visual processing. *Abstracts of the proceedings of the twelfth annual meeting of the Society of Magnetic Resonance in Medicine*. Berkeley: Society of Magnetic Resonance in Medicine; 1993;1:56.
 40. DeYoe EA, Neitz J, Miller D, Wiesner J. Functional magnetic resonance imaging (fMRI) of visual cortex in human subjects using a unique video graphics stimulator. *Abstracts of the proceedings of the twelfth annual meeting of the Society of Magnetic Resonance in Medicine*. Berkeley: Society of Magnetic Resonance in Medicine; 1993;3:1394.
 41. Tootell RBH, Kwong KK, Belliveau JW, et al. Functional MRI (fMRI) evidence for MT/V5 and associated cortical areas in man. *Abstracts of the proceedings of the twenty-third annual meeting of the Society for Neuroscience*. 1993;1:618.9.
 42. Karni A, Ungerleider L, Haxby J, et al. Stimulus dependent MRI signals evoked by oriented line-element textures in human visual cortex. *Abstracts of the proceedings of the twenty-third annual meeting of the Society for Neuroscience*. Washington, D.C.: Society for Neuroscience, 1993;1:618.11.
 43. Sorensen AG, Caramia F, Wray SH, et al. Extrastriate activation in patients with visual field defects. *Abstracts of the proceedings of the twelfth annual meeting of the Society of Magnetic Resonance in Medicine*. Berkeley: Society of Magnetic Resonance in Medicine; 1993;1:62.
 44. Binder JR, Rao SM, Hammeke TA, et al. Functional magnetic resonance imaging (fMRI) of auditory semantic processing. *Neurology* 1993;43(Suppl 2):A189.
 45. Binder JR, Rao SM, Hammeke TA, et al. Lateralized human brain language systems demonstrated by task subtraction functional magnetic resonance imaging. *Arch Neurol* 1995 [In press].
 46. Cohen JD, Forman SD, Casey BJ, Noll DC. Spiral-scan imaging of dorsolateral prefrontal cortex during a working memory task. *Abstracts of the proceedings of the twelfth annual meeting of the Society of Magnetic Resonance in Medicine*. Berkeley: Society of Magnetic Resonance in Medicine; 1993;3:1405.
 47. Blamire AM, McCarthy G, Puce A, et al. Functional magnetic resonance imaging of human pre-frontal cortex during a spatial memory task. *Abstracts of the proceedings of the twelfth annual meeting of the Society of Magnetic Resonance in Medicine*. Berkeley: Society of Magnetic Resonance in Medicine; 1993;3:1413.
 48. Frahm J, Merboldt KD, Hänicke W, Kleinschmidt A, Steinmetz H. High-resolution functional MRI of focal subcortical activity in the human brain. Long-echo time FLASH of the lateral geniculate nucleus during visual stimulation. *Abstracts of the proceedings of the twelfth annual meeting of the Society of Magnetic Resonance in Medicine*. Berkeley: Society of Magnetic Resonance in Medicine; 1993;1:57.
 49. Kim S-G, Ashe J, Hendrich K, et al. Functional magnetic resonance imaging of motor cortex: Hemispheric asymmetry and handedness. *Science* 1993;261:615-616.
 50. Connelly A, Jackson GD, Cross JH, Gadian DG. Functional magnetic resonance imaging of focal seizures. *Abstracts of the proceedings of the twelfth annual meeting of the Society of Magnetic Resonance in Medicine*. Berkeley: Society of Magnetic Resonance in Medicine; 1993;1:61.
 51. Wong EC, Bandettini PA, Hyde JS. Echo-planar imaging of the human brain using a three axis local gradient coil. *Abstracts of the proceedings of the eleventh annual meeting of the Society of Magnetic Resonance in Medicine*. Berkeley: Society of Magnetic Resonance in Medicine; 1992;1:105.
 52. Wong EC, Boskamp E, Hyde JS. A volume optimized quadrature elliptical endcap birdcage brain coil. *Abstracts of the proceedings of the eleventh annual meeting of the Society of Magnetic Resonance in Medicine*. Berkeley: Society of Magnetic Resonance in Medicine; 1992;3:4015.
 53. Bandettini PA, Jesmanowicz A, Wong EC, Hyde JS. Processing strategies for time-course data sets in functional MRI of the human brain. *Magn Reson Med* 1993;30:161-173.
 54. Penfield W, Boldrey E. Somatic motor and sensory representation in the cerebral cortex of man as studied by electrical stimulation. *Brain* 1937;60:389-443.
 55. Grafton ST, Woods RP, Mazziotta JC, Phelps ME. Somatotopic mapping of the primary motor cortex in humans: Activation studies with cerebral blood flow and positron emission tomography. *J Neurophysiol* 1991;66:735-743.
 56. Cao Y, Towle V, Levin DN, Grzeszczuk R, Mullan JF. Conventional 1.5 T functional MRI localization of human hand sensorimotor cortex with intraoperative electrophysiologic validation. *Abstracts of the proceedings of the twelfth annual meeting of the Society of Magnetic Resonance in Medicine*. Berkeley: Society of Magnetic Resonance in Medicine; 1993;3:1417.
 57. Schieber MH, Hibbard LS. How somatotopic is the motor cortex hand area? *Science* 1993;261:489.
 58. Seitz RJ, Roland PE, Bohm C, Greitz T, Stone-Elander S. Motor

- learning in man: A positron emission tomographic study. *Neuroreport* 1990;1:57-60.
59. Deiber MP, Passingham RE, Colebatch JG, Friston KJ, Frackowiak RS. Cortical areas and the selection of movement: A study with positron emission tomography. *Exp Brain Res* 1991;84:393-402.
 60. Colebatch JC, Deiber MP, Passingham RE, Friston KJ, Frackowiak RS. Regional cerebral blood flow during voluntary arm and hand movements in human subjects. *J Neurophysiology* 1991;65:1392-1401.
 61. Orgogozo JM, Larson B. Activation of the supplementary motor area during voluntary movement in man suggests it works as a supramotor area. *Science* 1979;206:847-850.
 62. Roland PE, Meyer E, Shibasaki T, Yumamoto YL, Thompson CJ. Regional cerebral blood flow changes in cortex and basal ganglia during voluntary movements in normal human volunteers. *J Neurophysiol* 1982;48:467-478.
 63. Roland PE, Larsen B, Lassen NA, Skinhoj E. Supplementary motor area and other cortical areas in organization of voluntary movements in man. *J Neurophysiol* 1980;43:118-136.
 64. Roland PE, Skinhoj E, Lassen NA, Larsen B. Different cortical areas in man in organization of voluntary movements in extrapersonal space. *J Neurophysiol* 1980;43:137-150.
 65. Kim S-G, Ashe J, Georgopoulos AP, et al. Functional imaging of human motor cortex at high magnetic field. *J Neurophysiol* 1993;69:297.
 66. Van Essen DC, Newsome WT, Maunsell JHR. The visual field representations in striate cortex of the macaque monkey: Asymmetries, anisotropies, and individual variability. *Vision Res* 1984;24:429-448.
 67. Talbot SA, Marshall WH. Physiological studies on neuronal mechanisms of visual localization and discrimination. *Am J Ophthalmol* 1941;24:1255-1264.
 68. Tootell RBH, Switkes E, Silverman MS, Hamilton SL. Functional anatomy of macaque striate cortex. II. Retinotopic organization. *J Neurosci* 1988;8:1531-1588.
 69. Brindly GS, Lewin WS. The sensations produced by electrical stimulation of the visual cortex. *J Physiol* 1968;196:479-493.
 70. Dobelle WH, Mladejovsky MG. Phosphenes produced by electrical stimulation of human occipital cortex, and their application to the development of a prosthesis for the human occipital cortex. *J Physiol* 1974;243:553-576.
 71. Fox PT, Mintun MA, Raichle ME, Miezin FM, Allman JM, Van Essen DC. Mapping human visual cortex with positron emission tomography. *Nature* 1986;323:806-809.
 72. Fox PT, Miezin MA, Allman JM, Van Essen DC, Raichle ME. Retinotopic organization of human visual cortex mapped with positron emission tomography. *J Neurosci* 1987;7:913-922.
 73. Mora BN, Carman GJ, Allman JM. In vivo functional localization of the human visual cortex using positron emission tomography and magnetic resonance imaging. *Trends Neurosci* 1989;12:282-284.
 74. Liberman AM. Perception of the speech code. *Psychol Rev* 1967;74:431-461.
 75. Hari R. Activation of human auditory cortex by speech sounds. *Acta Otolaryngol* 1991;S491:132-138.
 76. Mazziotta JC, Phelps ME, Carson RE, Kuhl DE. Tomographic mapping of human cerebral metabolism: Auditory stimulation. *Neurology* 1982;32:921-937.
 77. Peterson SE, Fox PT, Posner MI, et al. Positron emission tomographic studies of the cortical anatomy of single-word processing. *Nature* 1988;331:585-589.
 78. Wise R, Chollet F, Hadar U, et al. Distribution of cortical neural networks involved in word comprehension and word retrieval. *Brain* 1991;114:1803-1817.
 79. Lauter J, Herscovitch P, Formby C, Raichle. Tonotopic organization of human auditory cortex revealed by positron emission tomography. *Hearing Res* 1985;20:199-205.
 80. Zatorre RJ, Evans AC, Meyer E, Gjedde A. Lateralization of phonetic and pitch discrimination in speech processing. *Science* 1992;256:846-849.

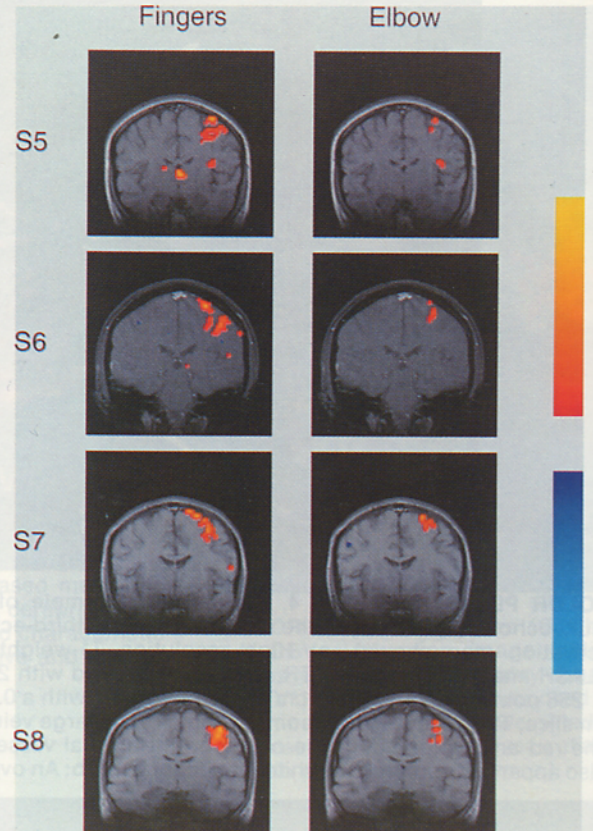
COLOR PLATES 19-22



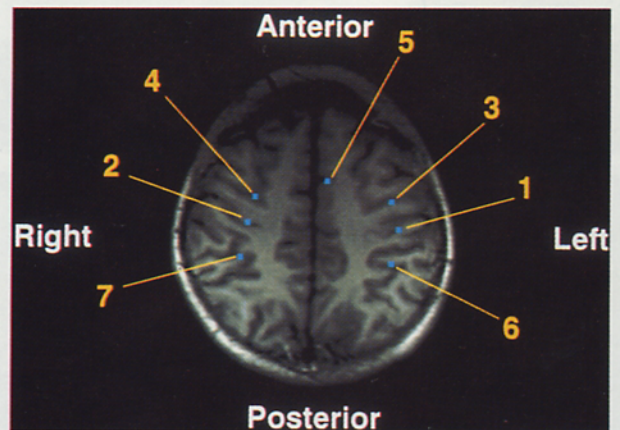
COLOR PLATE 19. (Figure 2, Chapter 19) Gradient and radiofrequency coil setup with subject.



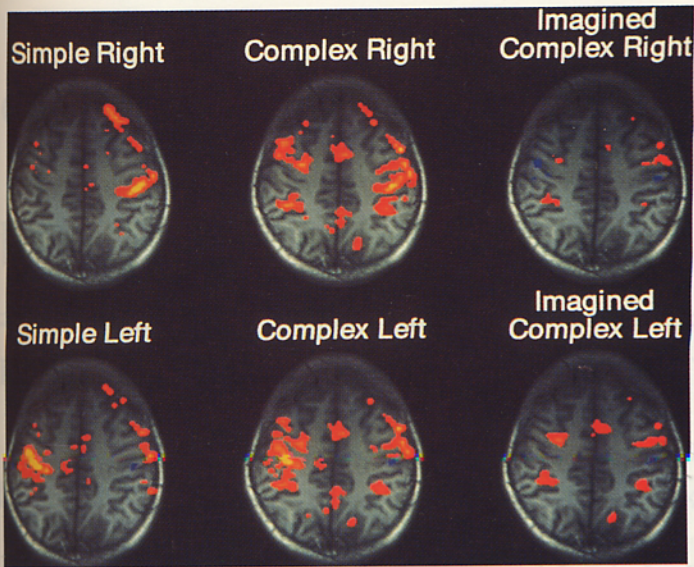
COLOR PLATE 20. (Figure 3, Chapter 19) Coronal functional images from four subjects comparing the regions of the motor strip activated by finger and toe movement. No spatial overlap was observed between finger and toe movement regions.



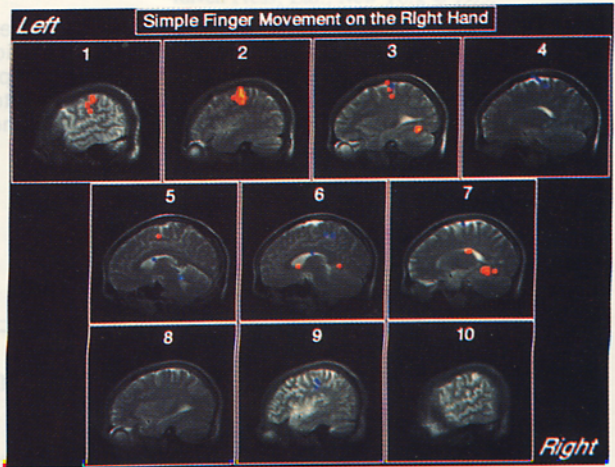
COLOR PLATE 21. (Figure 4, Chapter 19) Coronal functional images from four subjects comparing the regions of the motor cortex activated by finger and elbow movement. Some spatial overlap was observed between finger and elbow movement regions. Regions showing activation for elbow movement overlapped the more medial regions of activation for finger movement. In addition, the total area for elbow movements was smaller.



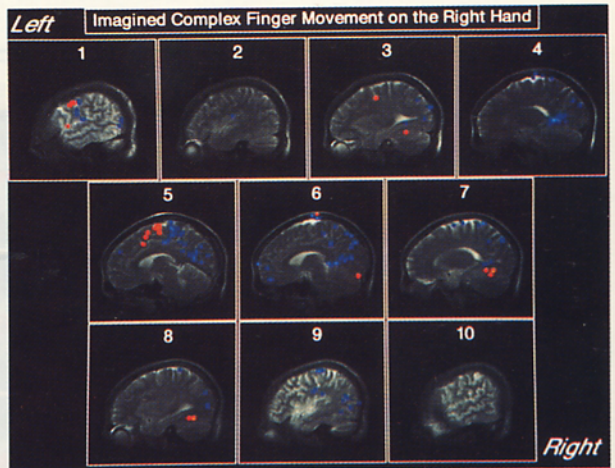
COLOR PLATE 22. (Figure 5, Chapter 19) High resolution image of the axial slice selected for a course study in which a subject performed simple, complex, and imagination of complex finger movements on each hand during different periods of the same time course. The time courses of the indicated regions are shown in Fig. 6 (Chapter 19).



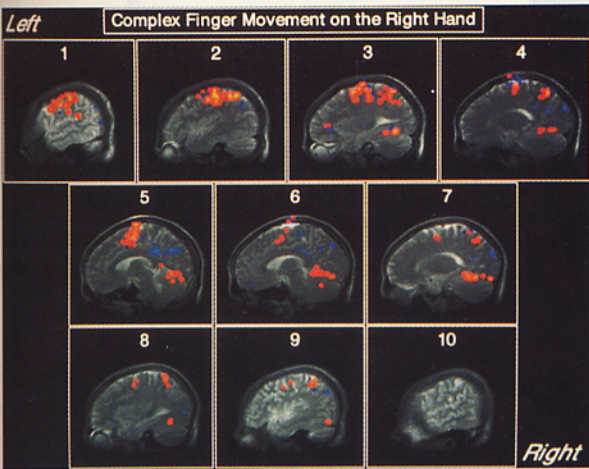
COLOR PLATE 23. (Figure 7, Chapter 19) Axial brain activation images created from the study shown in Figs. 5 (Color Plate 22) and 6 (Chapter 19). The images of simple, complex, and mental rehearsal of complex finger movement were created by temporal cross-correlation of a reference waveform with each of the six segments of the time course shown in Fig. 6 (Chapter 19).



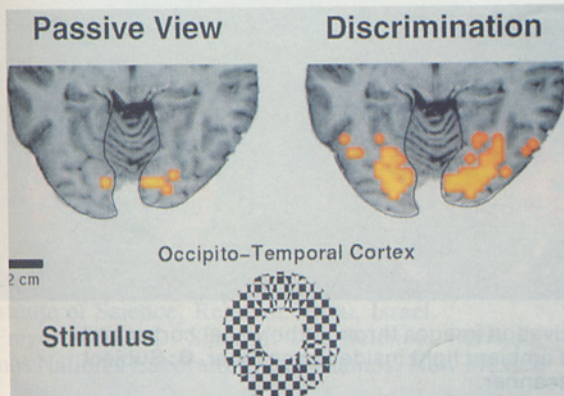
COLOR PLATE 24. (Figure 8, Chapter 19) Sagittal brain activation images containing the entire brain. Simple finger movement was performed on the right hand.



COLOR PLATE 26. (Figure 10, Chapter 19) Sagittal brain activation images containing the entire brain. Imagination of complex finger movement was performed on the right hand.

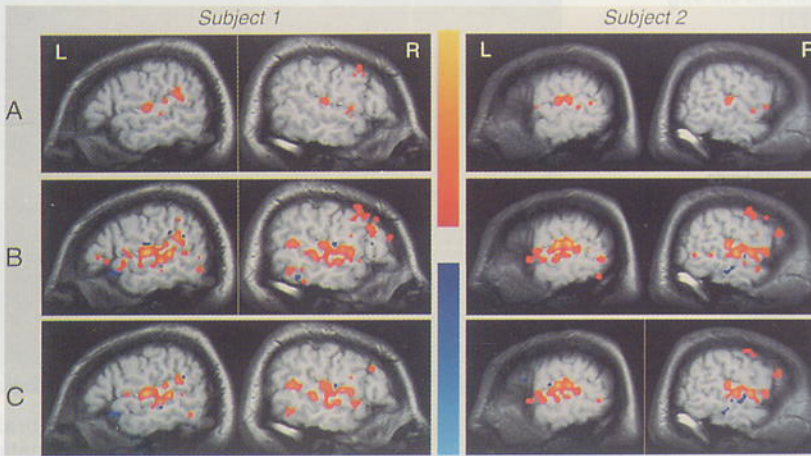
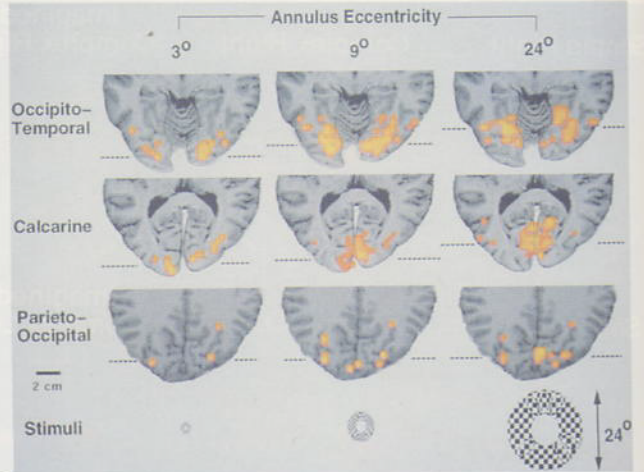


COLOR PLATE 25. (Figure 9, Chapter 19) Sagittal brain activation images containing the entire brain. Complex finger movement was performed on the right hand.

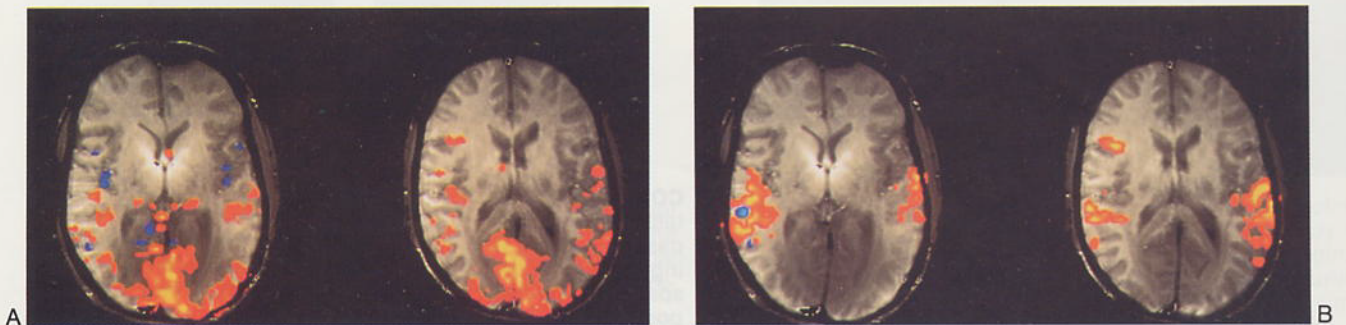


COLOR PLATE 27. (Figure 12, Chapter 19) Effect of visual task. Activation of striate and extrastriate cortex during a passive viewing task and an active discrimination task. During the active discrimination task the subject reported the spatial configuration of additional target patterns superimposed upon the checkerboard annuli. Discrimination caused more extensive activation outside the primary visual cortex. This is an example of how higher regions of the visual cortex can be mapped, not by altering the stimuli, but by altering the manner in which the subject must process the stimuli.

COLOR PLATE 28. (Figure 13, Chapter 19) Visual field mapping. Retinotopic mapping with active discrimination task. This allows simultaneous assessment of the retinotopic organization of striate and extrastriate cortex. The dotted lines on either side of each section are aligned with the major activity foci in each image.



COLOR PLATE 29. (Figure 14, Chapter 19) Sagittal images of the left and right temporal lobes of two subjects. Demonstrated are regions activated during passive listening to white noise (A), pseudowords (B), and words (C). The area activated by white noise was smaller than the area activated by either pseudowords or words. The area activated by pseudowords was generally the same size and shape as the area activated by words. (From the American Neurological Association, with permission.)



COLOR PLATE 30. (Figure 16, Chapter 19) Axial brain activation images through the visual cortex and temporal lobe. **A:** Subject was reading text, using only the ambient light inside the scanner. **B:** Subject was hearing words spoken through the intercom of the scanner.